JOURNAL OF Materials CHEMISTRY

Thermal and spectroscopic characterization of polypyrrole formed in zeolite Y

Hirofumi Uehara,[a] Michihiro Miyake,*[b]† Motohide Matsuda[b] and Mitsuo Sato[a]

[a]*Department of Chemistry, Faculty of Engineering, Gunma University, Tenjin, Kiryu 376, Japan*
[b]*Department of Environmental Chemistry and Materials, Faculty of Environmental Science and Technology, Tsushima-Naka, Okayama 700, Japan*

Encapsulation of pyrrole in two kinds of zeolite Y (NaY and USY) with various concentrations of Cu^{II} ions has been attempted by a gas diffusion process, and the products have been characterized by means of thermoanalytic and spectroscopic methods. From the results, it was found that the progress of polymerization depended on the Cu^{II} content, *i.e.* pyrrole was encapsulated as polypyrrole in both NaY and USY with a high concentration of Cu^{II} ions, and predominantly as pyrrole oligomer and/or monomer in those with a low concentration of Cu^{II} ions. Furthermore, EPR spectra revealed that NaY with a high concentration of Cu^{II} ions was active for the formation of bipolaron polypyrrole in the framework, whereas USY with a high concentration of Cu^{II} ions was not.

Introduction

As is well known, zeolite frameworks contain various kinds of channels and cages that are different in size and geometry. Recently, low-dimensional electric conductors synthesized in zeolites have attracted a great deal of attention for the creation of electronic devices with molecular dimensions. Intrazeolite synthesis of conducting polypyrrole was promoted by Bein *et al.*[1–4] and other research groups.[5–7] Bein *et al.* demonstrated the encapsulation of polypyrrole in the lattice space, using Cu^{II} or Fe^{III} ion-exchanged zeolite Y with three-dimensional channels and mordenite with one-dimensional channels, which were prepared from their sodium forms. Zeolite Y has 13 Å (supercage) pores with 7.4 Å windows formed by crossing of the channels. Roque *et al.* investigated oligomerization of pyrrole molecules occluded in Fe^{III} ion-exchanged proton-form zeolite Y.[5] McCann *et al.* suggested the presence of oligomers as well as long chain polymers in the channels of Cu^{II} ion-exchanged proton-form mordenite through a study on the encapsulation of pyrrole and thiophene.[7] The metallic ions introduced by the ion-exchange are used as oxidizing agents for the polymerization reaction. The relationships between the amount of oxidizing agent and the progress of polymerization in sodium-and proton-form zeolites were, however, hardly discussed in previous reports. It is of significance to clarify the relationships in order to design low-dimensional conductors in the lattice space of zeolites.

In this paper, we report the encapsulation of pyrrole in zeolite Y with various Cu^{II} contents as oxidizing agents and the characterization of the products synthesized in the lattice space. Zeolites Y used were the sodium and proton forms (NaY and USY), which exhibited octahedral-shaped crystallities with a size of about 50 μm. USY is an ultrastable form prepared from NaY by a dealumination procedure.

Experimental

NaY (HSZ-320NAA) and USY (HSZ-330HUA) were supplied by Tosoh Co. The Si/Al ratios are 2.7 in NaY and 3.0 in USY, respectively. Sodium and proton ions in zeolites were ion-exchanged with Cu^{II} ions at 50 °C for 48 h, using 1.0, 0.1, 0.01, and 0.001 mol dm^{-3} aqueous solutions of $Cu(NO_3)_2$. The ion-exchanged zeolites (1.0Cu-NaY, 0.1Cu-NaY, 0.01Cu-NaY, 0.001Cu-NaY, 1.0Cu-USY, 0.1Cu-USY, 0.01Cu-USY, and 0.001Cu-USY) and ion-unexchanged zeolites (0.0Cu-NaY and 0.0Cu-USY) were calcined at 500 °C for 2 h to eliminate zeolitic water. After cooling to 100 °C, pyrrole molecules were loaded by means of a gas diffusion process for 2 h. Then, the samples were evacuated for 2 h to remove excess pyrrole molecules adsorbed on the surface of the zeolites. Calcination and encapsulation were continuously carried out in the closed system without exposing the zeolites to the air.

The chemical compositions of the ion-exchanged zeolites were estimated by electron-probe microanalysis (EPMA), using a JEOL JXA-733 instrument. The thermal analysis (TG–DTA) was carried out in air at a heating rate of 10 °C min^{-1} up to 1000 °C, using a Rigaku TAS-100 instrument. The spectroscopic characterizations were made in three ways: (1) FTIR spectra by the KBr disk method in the range 4000–400 cm^{-1}, using a JASCO FT/IR 350 spectrometer, (2) UV–VIS absorption spectra in the range 250–800 nm, using a Shimazu UV-2100PC spectrometer, and (3) EPR spectra in X-band mode at room temperature, using a JEOL JES-RE2X instrument. The samples were compacted into disks in order to measure electric conductivities by the complex admittance method in the range 0.1–1000 kHz at room temperature. Gold films as electrodes were deposited upon both sides of the disk.

Results and Discussion

The chemical compositions of Cu^{II} ion-exchanged zeolites are given in Table 1. Cu^{II} contents in both NaY and USY increased with increasing the concentration of the $Cu(NO_3)_2$ aqueous solution used in the ion-exchange experiments. In addition, the Si/Al ratio in USY increased. It is said that dealuminated

Table 1 Chemical composition of Cu^{II}-exchanged zeolites

zeolite	Cu^{II} solution/mol dm^{-3}	chemical composition
Cu-NaY	1.0	$Cu_{20.1}Na_{16.3}Al_{49.8}Si_{142.2}O_{384}$
	0.1	$Cu_{17.7}Na_{19.8}Al_{53.7}Si_{138.3}O_{384}$
	0.01	$Cu_{13.6}Na_{34.9}Al_{50.9}Si_{141.1}O_{384}$
	0.001	$Cu_{2.5}Na_{60.7}Al_{50.9}Si_{141.1}O_{384}$
Cu-USY	1.0	$Cu_{12.3}H_{7.9}Al_{32.0}Si_{160.0}O_{384}$
	0.1	$Cu_{3.7}H_{33.7}Al_{41.1}Si_{150.9}O_{384}$
	0.01	$Cu_{1.5}H_{42.8}Al_{45.8}Si_{146.2}O_{384}$
	0.001	$Cu_{0.4}H_{46.7}Al_{47.5}Si_{144.5}O_{384}$

†E-mail: mmiyake@cc.okayama-u.ac.jp

zeolite generally contains extra-framework Al species.[8] The increase in the Si/Al ratio was, therefore, elucidated to be due to the elimination of extra-framework Al species from USY by treatment with high concentrations of $Cu(NO_3)_2$ aqueous solution.

The colors of the zeolites turned to light blue upon the ion-exchange treatment. After diffusion of pyrrole, marked color changes to black were observed, indicating the occurrence of some oxidative polymerization, since the color of bulk polypyrrole prepared by chemical polymerization is black.[9] The colors of 0.0Cu-NaY and 0.0Cu-USY were, however, not blackened upon contact with pyrrole.

Fig. 1 and 2 show FTIR spectra of Cu-NaY and Cu-USY

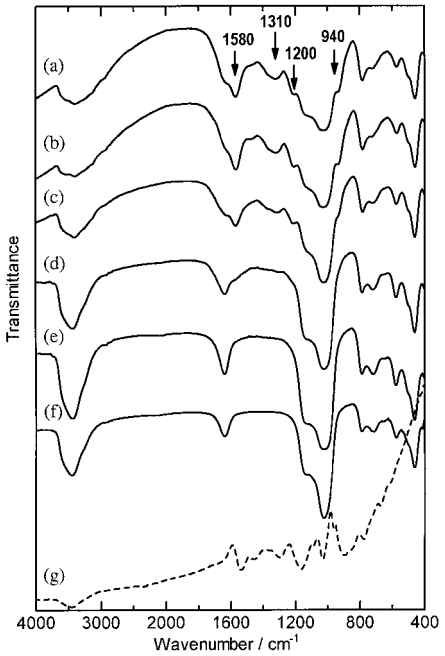

Fig. 1 FTIR spectra of (a) pyrrole/1.0Cu-NaY, (b) pyrrole/0.1Cu-NaY, (c) pyrrole/0.01Cu-NaY, (d) pyrrole/0.001Cu-NaY, (e) pyrrole/0.0Cu-NaY, (f) NaY and (g) bulk polypyrrole

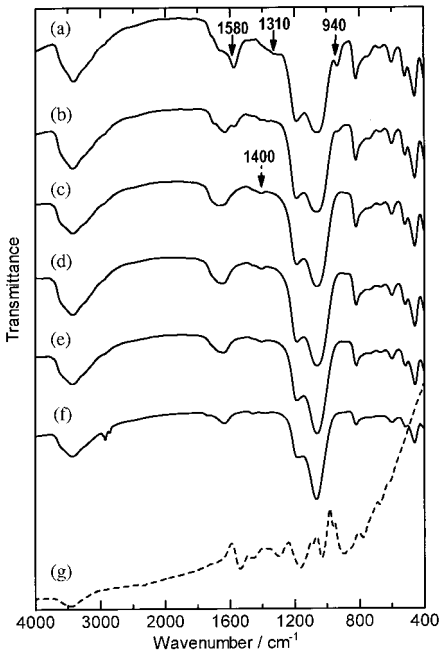

Fig. 2 FTIR spectra of (a) pyrrole/1.0Cu-USY, (b) pyrrole/0.1Cu-USY, (c) pyrrole/0.01Cu-USY, (d) pyrrole/0.001Cu-USY, (e) pyrrole/0.0Cu-USY, (f) USY and (g) bulk polypyrrole

with encapsulated pyrrole (pyrrole/Cu-NaY and pyrrole/Cu-USY), respectively. New IR bands were clearly observed in the spectra of pyrrole/1.0Cu-, 0.1Cu-, 0.01Cu-NaY, 1.0Cu-, and 0.1Cu-USY, as seen in Fig. 1(a)–(c) and 2(a), (b). These new absorption peaks were assigned as corresponding to characteristic bands of polypyrrole, although certain shifts of the IR bands towards higher wavenumbers were observed. The shifts were found to vary with host and preparation conditions.[1] Absorption peaks of the encapsulated materials, which were extracted from pyrrole/1.0Cu-NaY and -USY by dissolving the hosts in HF, were in agreement with those of bulk polypyrrole. The absorption peaks of polypyrrole could be distinguished from those of pyrrole oligomer and monomer existing in the host, because the former are relatively broad. Intensities of the characteristic peaks of polypyrrole decreased, and a new peak appeared around 1400 cm^{-1}, as seen in Fig. 2(c) and (d), which was assigned as corresponding to pyrrole oligomer and/or monomer, because the wavenumber of the 1400 cm^{-1} peak was close to that of the IR peak emerging as a consequence of the adsorption of pyrrole on acidic solids,[10] as seen in Fig. 2(e). Thus, pyrrole molecules were considered to be predominantly occluded as oligomers and/or monomers in pyrrole/0.01Cu- and 0.001Cu-USY. On the other hand, the 1400 cm^{-1} peak was indistinct in the FTIR spectrum of pyrrole/0.001Cu-NaY, and no significant differences between the FTIR spectra of pyrrole/0.001Cu- and 0.0Cu-NaY could be observed in the range 1600–900 cm^{-1} as seen in Fig. 1(d) and (e).

DTA curves of pyrrole/Cu-NaY and -USY are shown in Fig. 3 and 4, respectively. Exothermic peaks on the curves of pyrrole/Cu-NaY and -USY, which were assigned to the combustion of loaded pyrrole, broadened with decreasing Cu^{II} contents. Broad endothermic peaks were observed on the curves of pyrrole/0.0Cu-NaY and -USY, too, suggesting that pyrrole was fixed in these samples. The exothermic peaks for pyrrole/Cu-USY appeared in a higher temperature range than those for pyrrole/Cu-NaY. The thermal stability of pyrrole occluded in the lattice space was assumed to be affected by the strength of acidity in the cavity, from the remarkable difference between pyrrole/Cu-NaY and -USY. The weight losses of the samples in the range from 200–600 °C were observed to be about 5–23 mass%.

UV–VIS spectra of pyrrole/Cu-NaY and pyrrole/Cu-USY measured by diffuse reflectance are shown in Fig. 5 and 6, respectively. UV–VIS spectra of pyrrole/1.0Cu-, 0.1Cu- and

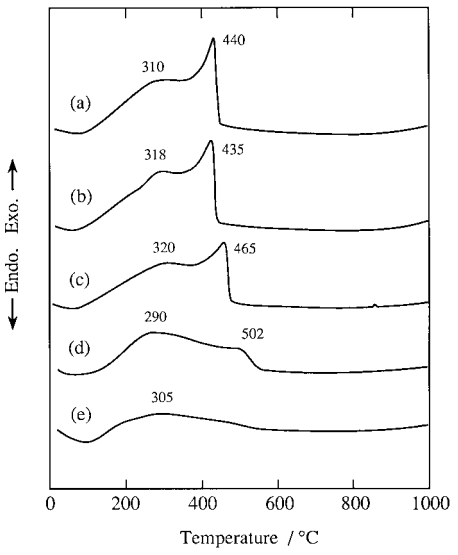

Fig. 3 DTA curves of (a) pyrrole/1.0Cu-NaY, (b) pyrrole/0.1Cu-NaY, (c) pyrrole/0.01Cu-NaY, (d) pyrrole/0.001Cu-NaY and (e) pyrrole/0.0Cu-NaY

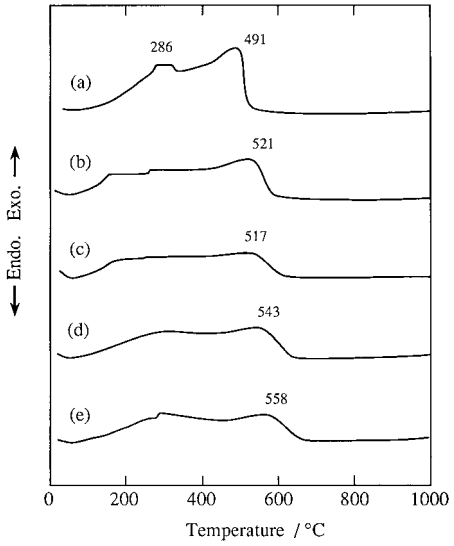

Fig. 4 DTA curves of (a) pyrrole/1.0Cu-USY, (b) pyrrole/0.1Cu-USY, (c) pyrrole/0.01Cu-USY, (d) pyrrole/0.001Cu-USY and(e) pyrrole/0.0Cu-USY

0.01Cu-NaY showed maxima at about 480 nm (*ca.* 2.6 eV) and 380 nm (*ca.* 3.3 eV), as seen in Fig. 5(a)–(c). On the other hand, the UV–VIS spectrum of pyrrole/0.001Cu-NaY showed maxima at about 450 nm (*ca.* 2.8 eV) and 340 nm (*ca.* 3.7 eV), as seen in Fig. 5(d), and that of pyrrole/0.0Cu-NaY showed no maximum. The different peak positions were considered to correspond to the situation of pyrrole in zeolites. The peak positions in the UV–VIS spectrum of pyrrole/1.0Cu-USY were close to those of pyrrole/1.0Cu-, 0.1Cu- and 0.01Cu-NaY. The peak positions in the UV–VIS spectra of pyrrole/0.1Cu-, 0.01Cu-, 0.001Cu- and 0.0Cu-USY were close to those of pyrrole/0.001Cu-NaY, though the intensities of the maxima increased. From the results of FTIR, DTA and UV–VIS data, it was concluded that polypyrrole was formed in pyrrole/1.0Cu-, 0.1Cu-, 0.01Cu-NaY, and 1.0Cu-USY, whereas pyrrole oligomer and/or monomer predominantly existed in pyrrole/0.001Cu-, 0.0Cu-NaY, 0.01Cu-, 0.001Cu-, and 0.0Cu-

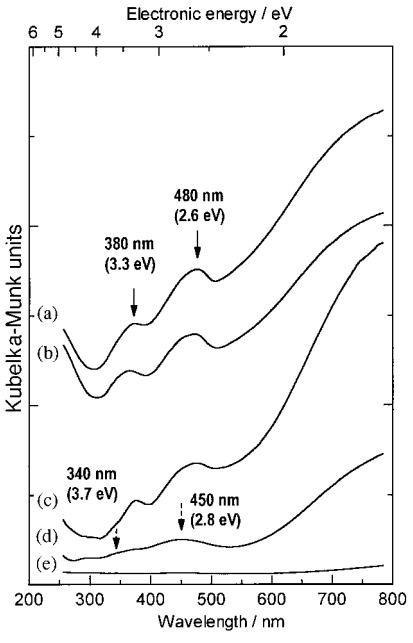

Fig. 5 UV–VIS spectra of (a) pyrrole/1.0Cu-NaY, (b) pyrrole/0.1Cu-NaY, (c) pyrrole/0.01Cu-NaY, (d) pyrrole/0.001Cu-NaY and (e) pyrrole/0.0Cu-NaY

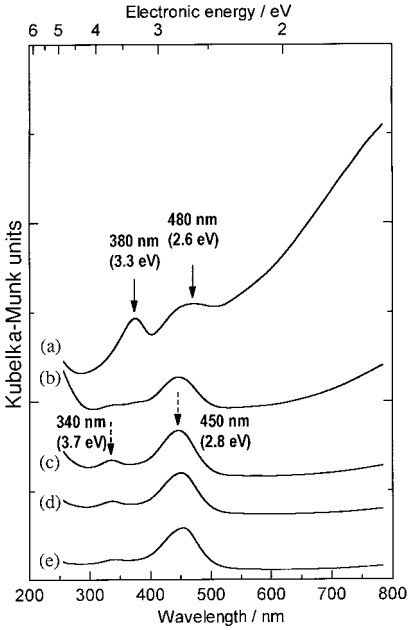

Fig. 6 UV–VIS spectra of (a) pyrrole/1.0Cu-USY, (b) pyrrole/0.1Cu-USY, (c) pyrrole/0.01Cu-USY, (d) pyrrole/0.001Cu-USY and (e) pyrrole/0.0Cu-USY

USY, and polypyrrole coexisted with pyrrole oligomer and/or monomer in pyrrole/0.1Cu-USY.

By comparison with the UV–VIS spectrum of bulk-doped polypyrrole prepared by electrochemical oxidation,[11,12] the maxima at about 380 and 480 nm were assigned as corresponding to the band gap (ω_1) and the transition within the band (ω_2)[13] of polypyrrole formed in pyrrole/Cu-NaY and -USY, respectively. Consequently, the electronic states of polypyrrole in pyrrole/1.0Cu-, 0.1Cu-, 0.01Cu-NaY, and 1.0Cu-USY were postulated to be not neutral but polaron or bipolaron, although another transition within the band (ω_3),[13] which is characteristic of the polaron states, could not be distinctly observed.

Polaron states, which have radical cations, lead to a signal in the EPR spectrum.[14,15] EPR spectra of pyrrole/1.0Cu-,

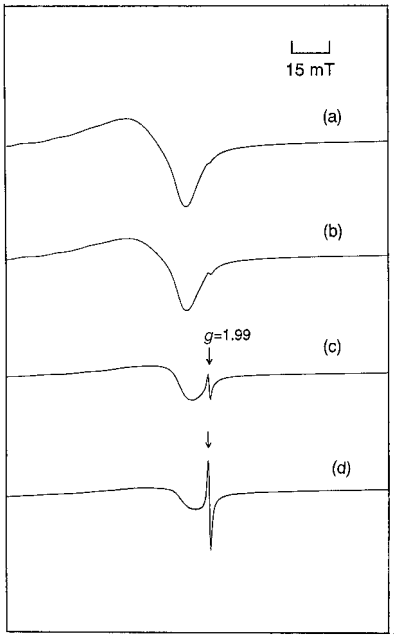

Fig. 7 EPR spectra of (a) pyrrole/1.0Cu-NaY, (b) pyrrole/0.1Cu-NaY, (c) pyrrole/0.01Cu-NaY and (d) pyrrole/1.0Cu-USY

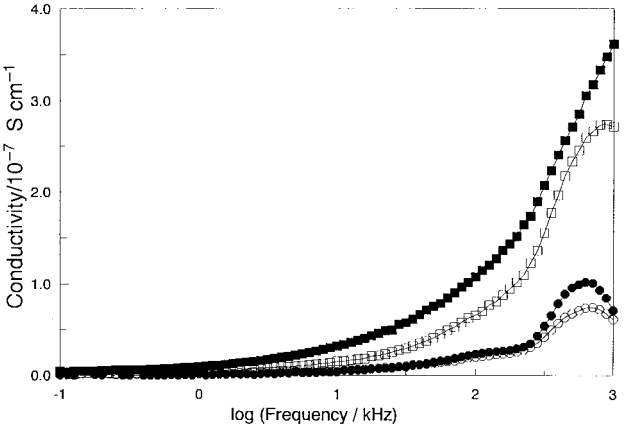

Fig. 8 Frequency dependences of electrical conductivities of pyrrole/1.0Cu-NaY (■), NaY (□), pyrrole/1.0Cu-USY(●), and USY (○)

0.1Cu-, 0.01Cu-NaY and 1.0Cu-USY, where polypyrrole was formed, are shown in Fig. 7. A new EPR signal at about $g=$ 1.99, which appeared after contact with pyrrole vapor, weakened with increasing Cu^{II} content on pyrrole/Cu-NaY, and was virtually absent in the spectrum of pyrrole/1.0Cu-NaY. As is well known, the coupling of polaron states produces bipolaron states, where an EPR signal is no longer observed. Thus, the reduction of EPR signals could be ascribed to evolution into bipolaron states. On the other hand, an EPR signal was noticeable in the spectrum of pyrrole/1.0Cu-USY, suggesting that there were some factors, *e.g.*, acidity, which inhibited the formation of the bipolaron states in pyrrole/1.0Cu-USY. The EPR signals were hardly altered by exposure of the samples to the atmosphere. It was, therefore, confirmed that polypyrrole formed in pyrrole/1.0Cu-NaY was in bipolaron states, while polypyrrole formed in pyrrole/1.0Cu-USY was in polaron as well as bipolaron states. Distinguishing features of bipolaron and polaron states could not be observed in UV–VIS spectra.

Cu^{II} ions were considered to be reduced to Cu^{I} ions by the encapsulation of polypyrrole, because of the decrease of the EPR signals of Cu^{II} ions. The total charge balance could be probably compensated by the generation of bipolaron (dication) and polaron (monocation) polypyrrole.

The electrical conductivities of NaY and USY were presumed to increase with polypyrrole loading in the lattice space, because polypyrrole is a conducting polymer. The frequency dependences of the electrical conductivities of NaY and USY before and after loading of polypyrrole are shown in Fig. 8. Significant differences of electrical conductivities before and after pyrrole loading were observed in the high frequency region, although the electrical conductivities were low. The low electrical conductivities were interpreted to be due to the fact that the electrodes on the powder-compacted disk did not come into complete contact with polypyrrole prepared in the lattice space. The electrical conductivity of pyrrole/1.0Cu-NaY was about four times higher than that of pyrrole/1.0Cu-USY in the high frequency region.

In conclusion, conducting polypyrrole was synthesized in pyrrole/1.0Cu-, 0.1Cu-, 0.01Cu-NaY, and 1.0Cu-USY, and the thermal stability of polypyrrole in pyrrole/Cu-USY was higher than that in pyrrole/Cu-NaY. It was found that the number of polaron states of polypyrrole formed in Cu-NaY decreased with increasing Cu^{II} content, and finally polypyrrole evolved into bipolaron states, whereas polypyrrole formed in pyrrole/1.0Cu-USY consisted of polaron states mixed with bipolaron states. On the other hand, polypyrrole as well as pyrrole oligomer and/or monomer existed in the other zeolites at low concentrations of Cu^{II} ions: namely polypyrrole and pyrrole oligomer and/or monomer were encapsulated in pyrrole/0.1Cu-USY, and pyrrole oligomer and/or monomer were mainly encapsulated in pyrrole/0.001Cu-, 0.0Cu-NaY, 0.01Cu-, 0.001Cu-, and 0.0Cu-USY.

This research was supported by Grant-in-Aid for Scientific Researches from the Ministry of Education, Science, and Culture of Japan.

References

1 T. Bein and P. Enzel, *Angew. Chem., Int. Ed. Engl.*, 1989, **28**, 1692.
2 T. Bein, P. Enzel, F. Beuneu and L. Zuppirioli, *Inorganic Compounds with Unusual Properties III. Electron Transfer in Biology and the Solid State*; *ACS Adv. Chem. Ser.*, 1990, **226**, 433.
3 S. Esnouf, F. Beuneu, J. Mory, L. Zuppiroli, P. Enzel and T. Bein, *J. Chim. Phys.-Chim. Biol.*, 1992, **89**, 1137.
4 L. Zuppiroli, F. Beuneu, J. Mory, P. Enzel and T. Bein, *Synth. Met.*, 1993, **55–57**, 5081.
5 R. Roque, J. de Onate, E. Reguera and E. Navarro, *J. Mater. Sci.*, 1993, **28**, 2321.
6 G. J. Millar, G. F. McCann, C. M. Hobbis, G. A. Bowmaker and R. P. Cooney, *J. Chem. Soc., Faraday Trans.*, 1994, **90**, 2579.
7 G. F. McCann, G. J. Millar, G. A. Bowmaker and R. P. Cooney, *J. Chem. Soc., Faraday Trans.*, 1995, **91**, 4321.
8 M. Stockenhuber and J. A. Lercher, *Microporous Mater.*, 1995, **3**, 457.
9 K. G. Neoh, T. C. Tan and E. T. Kang, *Polymer*, 1988, **29**, 553.
10 P. O. Scokart and P. G. Rouxhet, *J. Chem. Soc., Faraday Trans. 1*, 1980, **76**, 1476.
11 J. L. Bredas, J. C. Scott, K. Yakushi and G. B. Street, *Phys. Rev. B*, 1984, **30**, 1023.
12 J. L. Bredas and G. B. Street, *Acc. Chem. Res.*, 1985, **18**, 309.
13 J. H. Kaufman, N. Colaneri, J. C. Scott and G. B. Street, *Phys. Rev. Lett.*, 1984, **53**, 1005.
14 G. B. Street, T. C. Clarke, M. Krounbi, K. Kanazawa, V. Lee, P. Pfluger, J. C. Scott and G. Weiser, *Mol. Cryst. Liq. Cryst.*, 1982, **83**, 253.
15 J. C. Scott, P. Pfluger, M. T. Krounbi and G. B. Street, *Phys. Rev. B*, 1983, **28**, 2140.

Paper 8/04149K; *Received* 2nd *June*, 1998